J Mater Sci (2009) 44:2128–2136
DOI 10.1007/s10853-009-3307-0

Oxidation behavior of green coke-based carbon–ceramic composites incorporating micro- and nano-silicon carbide

Mandeep Kaur · Sandeep Kumar · P. R. Sengupta · V. Raman · G. Bhatia

Received: 18 August 2008 / Accepted: 30 January 2009 / Published online: 26 February 2009

Abstract The oxidation resistance of the carbon–ceramic composites developed using green coke-based carbon and carbon black as carbon source, boron carbide, and micro- and nano-silicon carbide was carried out in the temperature range of 800 to 1,200 °C. Silicon carbide particulate as such and silicon carbide obtained by the reaction of green coke and silicon provided micro silicon carbide while silicon and carbon black and sol–gel silica and carbon black used as silicon carbide precursors led to the formation of nano-silicon carbide. The oxidation resistance of these composites at 800 to 1,200 °C for 10 h showed that the size of the silicon carbide influenced the oxidation resistance. The weight gain due to protective coating formed on oxidation was higher in composites containing nano-silicon carbide as compared to the composites containing micro silicon carbide.

Introduction

Carbon-based materials like graphite and carbon–carbon composites have many potential applications in aerospace, defense, and industrial sectors due to their unique properties like light weight, high strength, high corrosion resistance, and high thermal conductivity [1]. The use of these materials for high temperature application is limited due to their susceptibility to oxidation at temperatures as low as 450 °C. To devise the solution to this problem, many attempts were made to coat the carbon material with oxidation inhibitors and also to dope them with phosphorus and boron containing compounds [2–5]. The coating technique is known to suffer from the disadvantage of developing cracks on heating resulting from the mismatch of co-efficient of thermal expansion between the coating material and the substrate namely the carbon material, while the doping technique could protect oxidation only up to 700 °C. To overcome the above said problems and to develop oxidation resistant carbon material, incorporation of oxidation resistant carbides namely silicon carbide (SiC) and boron carbide (B_4C) into the substrate during their processing was tried and this method led to the development of oxidation resistant carbon–ceramic composites [6–8]. The authors have also developed carbon–ceramic composites by heating in inert atmosphere, NPL developed coal tar pitch-based green coke (GC), silicon (Si), and B_4C at 2,200 °C, which could withstand oxidation at 800–1,200 °C for about 10 h [9]. In the present investigation, the authors report the development of oxidation resistant C–SiC–B_4C composites through the in situ formation of nano-SiC in these composites using Si and carbon black (CB) and also sol–gel silica and CB as SiC precursors at the heat treatment temperature of 1,400 °C. In addition, carbon–ceramic composites developed using the same processing conditions with GC–SiC particulates (micro size) and B_4C and also with GC and Si, which also leads to the formation of micro-SiC and B_4C, were also studied for the oxidation resistance for comparison purpose.

Experimental

Nano-SiC was developed using Si and CB and the oxidation resistant carbon–ceramic composites containing

M. Kaur · S. Kumar · P. R. Sengupta · V. Raman · G. Bhatia (✉)
Division of Engineering Materials, National Physical Laboratory, Carbon Technology Unit, Dr. K.S. Krishnan Road, New Delhi 110012, India
e-mail: gbhatia@mail.nplindia.ernet.in

micro- and nano-SiC were developed using different types of routes, which are described below:

Development of nano-SiC (Batch A)

Carbon black and Si in mole ratio of 1:1 were ball milled in tungsten carbide (WC) jar for about 4–5 h and made into pellets using a phenolic resin (5%) as binder and heat treated up to 1,400 °C employing the heating rate of 100 °C/h up to 1,000 °C followed by 30 °C/h up to 1,400 °C in argon atmosphere and kept at 1,400 °C for 2 h and cooled to room temperature in argon atmosphere to obtain nano-SiC. The product was oxidized at 700 °C in air to determine the unreacted CB, if any, in the final product.

Development of C–nano-SiC–B_4C (Batches B-1 and B-2)

The GC was developed at NPL by suitable heat treatment of coal tar pitch, which was then ball milled into a fine powder. The characteristics of the coal tar pitch and GC are given in Table 1. Commercial rock Si of 99.1% purity (impurity contents as provided by the supplier are given in Table 2) was ball milled in a WC jar with 20 balls for about 6 h to get Si powder having particle size of 7 μm. The B_4C powder of purity 99% and size 2 μm whose chemical analysis (provided by the supplier) given in Table 3 was used in present studies. The GC powder, CB, Si, and B_4C powders were weighed in a definite proportion of 50.48:8.45:20:20 and 42:13:30:15 (by weight), respectively, to form two batches (B-1 and B-2), which were ball milled for 6 h in a high speed ball mill (250 rpm, power 20%). The mixture was molded into rectangular plates of the size 40 mm × 10 mm × 5 mm using a conventional hydraulic press at a pressure of 1,400 kg/cm^2. These green plates were carbonized at 1,000 °C in argon employing a heating rate of 20 °C/h up to 250 °C, 10 °C/h up to 750 °C, and 15 °C/h up to 1,000 °C. The carbonized plates were further heat treated up to 1,400 °C by employing the heating rate of 100 °C/h up to 1,000 °C and 30 °C/h up to 1,400 °C in argon atmosphere and kept at 1,400 °C for 2 h followed by cooling to room temperature in argon atmosphere to get C–nano-SiC–B_4C composites.

Table 1 Characteristics of precursor coal tar pitch and the resulting green coke

Characteristics	Precursor coal tar pitch	Green coke (92 mix)
Softening point (°C)	86.6	–
Specific gravity	1.27	–
Quinoline insoluble content (%)	0.2	96.8
Toluene insoluble content (%)	22.6	98.9
Coking yield (%)	43.8	90.2
Volatile matter (%)	56.2	8.8
Impurities in green coke % (EDAX)		
Iron		0.35
Silicon		0.34
Sulfur		0.44
Calcium		0.15

Table 2 Chemical analysis of rock silicon (Si)

Impurities	Quantity
Iron	0.75%
Aluminum	450 ppm
Nickel	5 ppm
Copper	30 ppm
Calcium	750 ppm
Zinc	50 ppm
Sodium	40 ppm
Boron	20 ppm
Titanium	50 ppm
Manganese	5 ppm
Phosphorous	Not detected

Table 3 Chemical analysis of boron carbide powder

Impurities	Quantity (%)
Boric oxide (B_2O_3)	<0.1
Iron	<0.5
Silicon	<0.25
Manganese	<0.02
Calcium	<0.01
Aluminum	<0.02
Titanium	<0.002
Copper	<0.002
Cobalt	<0.002

Development of C–nano-SiC–B_4C through sol–gel technique (Batch C)

Sol–gel silica was prepared by hydrolyzing tetraethylorthosilicate (TEOS) with rectified spirit, and water. TEOS, rectified spirit, and water were mixed in 1:4:4 ratios and stirred for about 8 h in the magnetic stirrer, to get silica sol, which was kept overnight for gelling. The silica gel thus was dried at 40 °C to get sol–gel silica. The sol–gel-derived silica was mixed with GC, CB, and B_4C powders in definite proportion (Table 6, Batch C) and ball milled for 6 h using WC jar in a high speed ball mill. The mixture so obtained was molded into plates of 40 mm × 10 mm × 5 mm size, carbonized and heat treated up to 1,400 °C in argon gas as in the case of Batch B to get C–nano-SiC–B_4C composites.

Development of C–micro-SiC–B_4C using green coke (GC), Si or SiC, B_4C powders (Batches D-1, D-2, E-1, and E-2)

Two batches D-1 and D-2 containing weight proportion of 60:20:20 and 55:30:15 of GC, Si, and B_4C as well as two other batches E-1 and E-2 containing weight proportion of 50:28.6:20 and 40.7:42.9:15 of GC, SiC (7 μm), and B_4C powders, respectively, were prepared and ball milled in separate lots, molded into plates of 40 mm × 10 mm × 5 mm size. The green plates were then heat treated as mentioned above to 1,000 °C and then to 1,400 °C in argon as mentioned above to get C–micro-SiC–B_4C composites.

Characterization

The SiC prepared by the reaction between Si and CB (Batch A) and the C–SiC–B_4C composites (Batches B-1, C and D-1) developed were characterized by X-ray diffraction technique employing D-8 Advanced Bruker Powder X-ray diffractometer using CuKα radiation ($\lambda = 1.5418$ Å) spectrometer. The surfaces of nano-SiC (Batch A) oxidized at 800, 1,000, and 1,200 °C were also examined by XRD technique. The surface morphology of the samples was determined by scanning electron microscopy (SEM, LEO-440) and transmission electron microscopy (TEM, Jeol JEM 2000 CX).

The oxidation resistance studies of the carbon–ceramic composites so developed were carried out by cutting specimen of size 12 mm × 3 mm × 5 mm from the composites. The samples specimen were first heated up to the required temperatures (800, 1,000, and 1,200 °C) in argon followed by heating in air for the specified period (5, 10 h) and then cooled in argon up to room temperature and weighed again to observe the weight change. The SiC pellets prepared by heat treatment of Si and CB (Batch A) were also subjected to oxidation resistant studies at 800–1,200 °C to see the effect of oxidation on nano-SiC.

Results and discussion

Characteristics of precursors

The characteristics of the coal tar pitch and the GC derived from it are given in Table 1. It is seen from the Table 1 that precursor coal tar pitch had a low quinoline insolubles (QI) content (0.2%), low toluene insolubles (TI) content (22.6%), and low coking yield (43.8%) compared to self-sintering GC powder having high QI content (96.8%), high TI content (98.9%), and high coking yield (90.2%). This is due to the removal of volatile matter (on pyrolysis to 470 °C) and also the polymerization and condensation reactions taking place among the various molecular species of the coal tar pitch. Thus, volatile matter was reduced from a value of about 56.2% for the precursor coal tar pitch to a value of 8.8% for the self-sintering (GC) powder.

It is seen from Table 1 that the GC also contained impurities like iron and Si, which could have been introduced into it from the metallic equipment employed during the processing of coal tar pitch. The impurities present in Si and B_4C used in the present investigations are given in Tables 2 and 3, respectively. It is seen from these values given in Tables 2 and 3 that Si also contained metallic impurities while B_4C had both metallic as well as boric oxide impurities. The impurities especially iron and boric oxide could influence both the melting of Si and the formation of nano-SiC.

X-ray analysis

The X-ray patterns of nano-SiC derived by the reaction between Si and CB and of different composite materials (Batches A, B-1, C and D-1) are given in Fig. 1a–d. The patterns showed characteristic peaks of β-SiC at $2\theta = 35.5°$, 60°, and 72° confirming the formation of β-SiC by the reaction between Si and CB (Batch A and Batch B-1), sol–gel silica, and CB (Batch C) and also between Si and GC (Batch D-1). The X-ray patterns (Fig. 1a) of SiC (Batch A) derived by the reaction of Si and CB alone did not show characteristic peaks either due to excess carbon or Si thereby showing that both the CB and Si had completely reacted. This is also in agreement with recent results of Prabhakaran et al. [10] who also observed that the X-ray powder patterns of nano to sub-micron size SiC prepared by heat treating phenol-furfuraldehyde and Si did not reveal peaks either due to Si or resin-derived carbon, which indicates that complete reaction takes place between Si and the carbon source provided stoichiometric quantities of Si powder and carbon are employed for the synthesis of SiC.

Oxidation resistance studies

The results of the oxidation resistance studies on SiC developed using Si and CB (Batch-A) and of commercial SiC powder (7 μm) are shown in Table 4. The oxidation resistance of carbon–ceramic composites developed with GC–CB–Si–B_4C (Batches B-1 and B-2), GC–CB–sol gel silica–B_4C (Batch C), GC–Si–B_4C (Batches D-1 and D-2), and GC–SiC–B_4C (Batches E-1 and E-2) are given in Tables 5, 6, 7, and 8, respectively. It is seen from the values listed in these tables that all the composites developed by taking different precursors for SiC showed weight gain on oxidation at 800 °C instead of weight loss. The

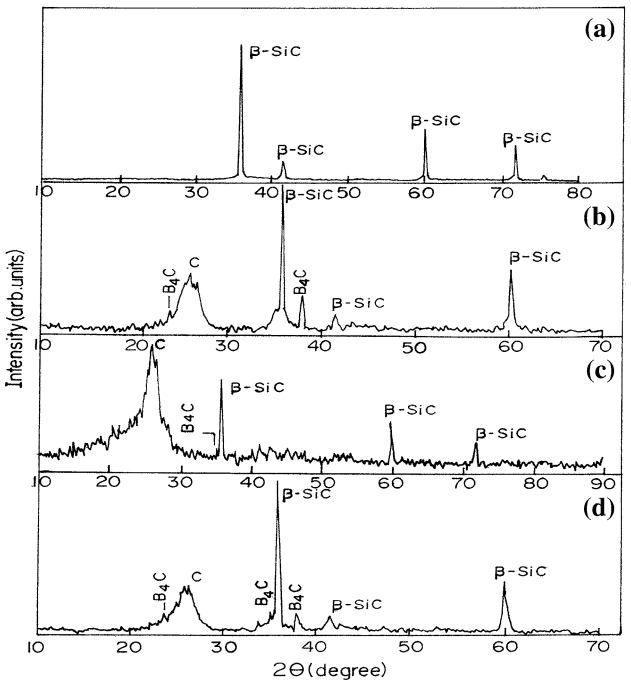

Fig. 1 X-ray diffraction pattern of **a** SiC synthesized from Si and CB (Batch A), **b** C–nanoSiC–B_4C (Batch B-1, nano-SiC derived from Si and CB), **c** C–nano-SiC–B_4C (Batch C, nano-SiC derived from sol–gel silica and CB) and **d** C–micro-SiC–B_4C (Batch D-1, micro-SiC derived from Si and GC)

weight gain is due to the formation of B_2O_3 [9, 11, 12] by the oxidation of B_4C in air according to the reaction.

$$B_4C + 4O_2 \rightarrow 2B_2O_3 + CO_2. \quad (1)$$

It is also seen that the weight gain during oxidation at 800 °C for 10 h is more in composites developed with Si–CB (Batch B-1) and sol–gel silica–CB as SiC precursors (Batch C), i.e., 2.82% and 1.26%, respectively, as compared to the one developed with Si–GC (as SiC precursor Batch D-1) and SiC powder (Batch E-1), i.e., 0.75% and 0.26%, respectively. The increase in the weight gain in the composites developed with CB as carbon source for SiC may be attributed to the formation of nano-SiC since all other constituents are the same in these composites except the SiC precursors. This observation is supported by the weight gain of the 0.47% observed on the oxidation of nano-SiC pellet (Batch A) at 800 °C for 10 h (Table 4). It also appears from the values given in Tables 5, 6, 7, and 8 that the smaller the size of SiC greater is the weight gain. This observation is supported by the SEM and TEM

Table 5 Oxidation resistance of carbon–ceramic composites using Si, GC, and CB as SiC precursor

Batch	Composition (g)	Weight change (%)		
		800 °C	1,000 °C	1,200 °C
B-1	GC–CB–Si–B_4C	2.34 (5 h)	0.43 (5 h)	−0.61 (5 h)
	50.48–8.45–20–20	2.82 (10 h)	0.41 (10 h)	−0.71 (10 h)
B-2	GC–CB–Si–B_4C	3.84 (5 h)	2.9 (5 h)	2.88 (5 h)
	42–13–30–15	4.48 (10 h)	2.95 (10 h)	3.27 (10 h)

Table 6 Oxidation resistance of carbon–ceramic composite using sol–gel silica, GC, and CB as SiC precursor

Batch	Composition (g)	Weight change (%)		
		800 °C	1,000 °C	1,200 °C
C	GC–CB–SiO_2–B_4C	1.16 (5 h)	−6.97 (5 h)	−7.66 (5 h)
	25–4.5–22–10	1.26 (10 h)	−7.25 (10 h)	−7.83 (10 h)

Table 7 Oxidation resistance of carbon–ceramic composites using Si and GC as SiC precursor

Batch	Composition (g)	Weight change (%)		
		800 °C	1,000 °C	1,200 °C
D-1	GC–Si–B_4C	0.63 (5 h)	0.38 (5 h)	0.33 (5 h)
	60–20–20	0.75 (10 h)	0.35 (10 h)	0.33 (10 h)
D-2	GC–Si–B_4C	0.81 (5 h)	0.66 (5 h)	0.62 (5 h)
	55–30–15	1.09 (10 h)	0.65 (10 h)	0.69 (10 h)

Table 8 Oxidation resistance of carbon–ceramic composites using SiC particulate

Batch	Composition (g)	Weight change (%)		
		800 °C	1,000 °C	1,200 °C
E-1	GC–SiC–B_4C	0.19 (5 h)	0.15 (5 h)	−0.28 (5 h)
	50–28.6–20	0.26 (10 h)	0.18 (10 h)	−0.36 (10 h)
E-2	GC–SiC–B_4C	0.17 (5 h)	0.14 (5 h)	0.37 (5 h)
	40.7–42.9–15	0.20 (10 h)	0.14 (10 h)	0.49 (10 h)

Table 4 Oxidation resistance of nano-SiC from Si and CB as SiC precursor and commercial micro-SiC powder

Batch	Composition (g)	Weight change (%)		
		800 °C	1,000 °C	1,200 °C
A	CB–Si	0.41 (5 h)	17.81 (5 h)	21.12 (5 h)
	24–56	0.47 (10 h)	20.22 (10 h)	24.74 (10 h)
Micron sized SiC	Commercial SiC powder (7 μm)	0.0 (5 h)	4.0 (5 h)	–

analysis (explained in detail under sub-heading SEM and TEM studies), which revealed that the size of nano-SiC with sol–gel silica and CB as SiC precursor in batch C is smaller than the SiC developed with Si and CB (Batch A and B-1); thereby confirming our above observation that the nano-SiC and their size influence the oxidation of composites. Further, it is learnt from the literature [13, 14] that nano-SiC is extremely sensitive to oxidation and due to its small radius gets oxidized at lower temperature (around 700 °C instead of 950 °C) to give silica, which also adds to the weight gain resulting from the oxidation of B_4C. To confirm this, SiC synthesized by reaction between Si and CB (Batch A) was also oxidized at 800 to 1,200 °C for 10 h and the results are given in Table 4. It is seen from the values listed in Table 4 that SiC (Batch A) on oxidation at 800, 1,000, and 1,200 °C showed a weight gain of 0.47, 20.22, and 24.74%, which indicate that due to the nano sized SiC the initiation of oxidation of SiC to SiO_2 starts around 700–800 °C and maximum amount of SiO_2 is formed around 1,000 °C:

$$\text{Micro SiC} + O_2 \overset{\text{Heat} > 950\,^{\circ}\text{C}}{\rightarrow} SiO_2 + CO_2 \uparrow, \quad (2)$$

$$\text{Nano SiC} + O_2 \overset{\text{Heat} > 700\,^{\circ}\text{C}}{\rightarrow} SiO_2 + CO_2 \uparrow . \quad (3)$$

It is important to mention here that micron SiC powder (7 μm) used in Batches E-1 and E-2 did not show any weight gain on oxidation at 800 °C for 5 h but exhibited 4% weight gain upon oxidation at 1,000 °C for 5 h (Table 4). This is in agreement with the observations of Quanli et al. [15] who reported the initiation temperature of oxidation of 1.2 μm sized SiC is around 843 °C with the weight gain of around 10–11% on oxidation at 1,100 °C for 2 h while the initiation temperature of oxidation for 0.2 μm sized SiC is 783 °C with the weight gain of 17–18% on oxidation at 1,100 °C for 2 h. The above results show that both the initiation temperature of oxidation and the reaction rate attributing to the weight gain due to the formation of SiO_2 are dependent on the radius of the SiC particles. Further these authors also observed that oxidation of nano-SiC is faster than the micro sized SiC and the weight gain of the nano-SiC powder was about three times that of micron sized SiC. The oxidation activation energy of nano sized SiC is lesser (82.64 $kJmol^{-1}$) than that (110.74 $kJmol^{-1}$) of micro-sized SiC and the weight gain due to oxidation of SiC increases with decreasing particle size of SiC powders. The weight gain at 800 °C due to the oxidation of nano sized SiC having the average particle size of 0.2 μm is around 1% as reported by Quanli et al. [15] and the weight gain value of 0.47% obtained in the present investigation on oxidizing nano sized SiC particles having average particle size of 0.4 μm (please see Fig. 3a) is very much in agreement with these results. To confirm the formation of SiO_2 through the oxidation of nano-SiC, the surfaces of the nano-SiC oxidized at 800 and 1,200 °C were subjected to X-ray studies and the patterns are given in Fig. 2a–c. It is seen from these pattern that the peak due to SiO_2 around $2\theta = 22°$ is not prominent in the nano-SiC oxidized at 800 °C (Fig. 2a) since the amount of SiO_2 formed at 800 °C is only 0.47% while the intensity of the peak attributable to SiO_2 at $2\theta = 22°$ increases with increase in the oxidation temperature and prominent peak due to SiO_2 were clearly visible in the X-ray patterns of the nano-SiC oxidized at 1,000 and 1,200 °C (Fig. 2b, c). All these results support the increased weight gain at 800 °C noticed in composite batches B-1, B-2, and C as compared to the weight gain observed on the oxidation of the composite batches D-1, D-2, E-1, and E-2. The weight gain is expected to be maximum in composites having CB and Si-derived nano-SiC, and thus the same is observed in this investigation. It is important to mention here that the weight gain in Batch C, which also has sol–gel-derived nano-SiC was lesser than the weight gain observed for Batch B, which is probably due to the incomplete formation of SiC in Batch C and also the oxidation of unreacted CB, which was accompanied by weight loss.

The oxidation of composites at 1,000 °C for 10 h also led to weight gain of 0.41%, 0.35%, and 0.18% in composite batches B-1, D-1, and E-1, respectively. This is

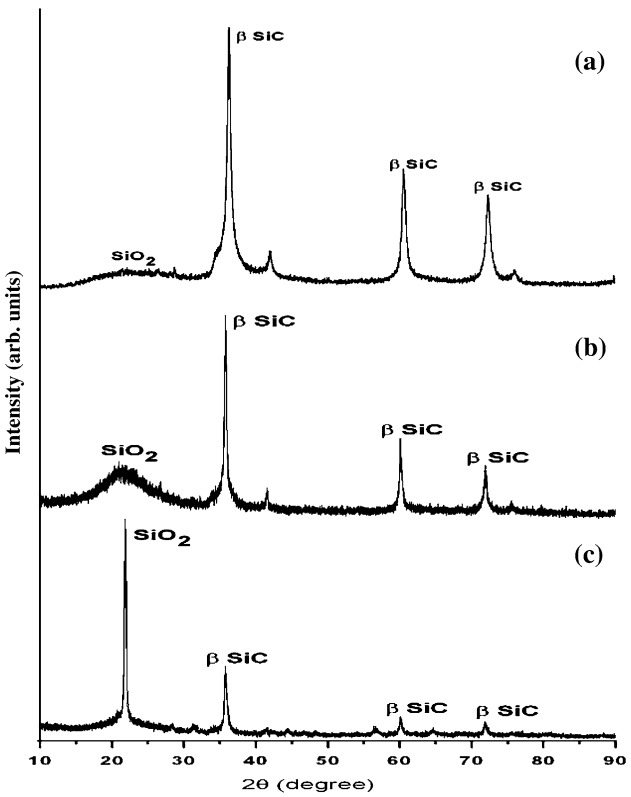

Fig. 2 Surface X-ray analysis of nano-SiC (Batch A) oxidized at **a** 800°C, **b** 1,000 °C, and **c** 1,200 °C

attributed to the combined effect of B_4C oxidation as explained above and to the partial decomposition of SiC into SiO_2 and CO_2, which is reported to start around 950 °C for micro-SiC and around 700 °C for nano-SiC [7, 9, 11, 14] as per the reaction

$$SiC + 2O_2 \rightarrow SiO_2 + CO_2. \quad (4)$$

The weight gain observed on oxidation of the composites (Batch B-1, B-2, D-1, D-2, E-1, and E-2) at 1,000 °C was less than the values obtained on oxidation at 800 °C. This difference in weight gain between 800 and 1,000 °C is due to the volatilization of B_2O_3 [11, 16, 17] formed from the oxidation of B_4C (Eq. 1). The composites developed with sol–gel silica (Batch C) showed 7.25% weight loss for 10 h at 1,000 °C (Table 6), which is due to the incomplete formation of SiC from sol–gel silica since unreacted carbon in the composite (CB) is expected to get oxidized leading to the weight loss, which is supported by our earlier observation in which the SiC-derived through sol–gel technique always contained unreacted carbon and silica [18, 19]. Further, it is noticed from the X-ray patterns of the composites (Batches B-1, C, and D-1) that the intensity of the carbon peak in the composite developed by using sol–gel silica as SiC precursor (Batch-C, Fig. 1c) was more as compared to the intensity of the carbon peaks observed in the X-ray patterns of batches B-1 and D-1 (Fig. 1b, d), which were developed using Si and CB and Si and GC as SiC precursors, respectively, and this increase in intensity for the carbon peak in the X-ray pattern of Batch C is due to the unreacted CB in the composite developed through sol–gel process.

The oxidation resistance of composites at 1,200 °C also followed the same trend. The weight loss was not significant for batches B-1 (0.71%) and E-1 (0.36%) for 10 h (Tables 5, 8). It is also seen from Table 6 (Batch C) that the weight loss was very high (7.83%) as compared to the values observed for B-1 and E-1, which is also attributed to the incomplete formation of nano-SiC that is expected to get oxidized to glassy layer of SiO_2 around 700 °C [16] and in turn will form protective glassy borosilicate layer around 1,200 °C. The incomplete formation of nano-SiC could not produce sufficient quantity of borosilicate layer to inhibit oxidation at 1,200 °C. The values listed in Table 5 for batch B-2, Table 7 for batches D-1 and D-2, and Table 8 for batch E-2 showed weight gain of 3.27%, 0.33%, 0.69%, and 0.49%, respectively, for 10 h. This weight gain in the case of composites D-1 and D-2 (0.33% and 0.69%) developed with Si is due to the formation of dense SiC through the melting of Si followed by its reaction with GC-based carbon. The weight gain observed in batch E-2 was due to the increased amount of SiC (42.9 gm) as compared to E-1 (28.6 gm) batch because in case of E-2 more quantity of SiO_2 will be formed on oxidation in the temperature range of 950 to 1,200 °C. It is observed from the values given for oxidation resistance at 1,200 °C for batches B-2, D-1, D-2, and E-2 that the weight gain is maximum in the case of B-2 (3.27%), which is attributed to the increased amount of Si added during processing (Table 5) of the composite that led to increased quantity of nano-SiC. It is already mentioned that in the case of nano-SiC, the oxidation of the SiC starts at lower temperature (700 °C) and it is completed around 1,000 °C (Table 4). The silicon oxide formed around 1,000 °C combines with B_2O_3 to form silica-rich borosilicate layer. These values also support our earlier observation that nano sized SiC formed in composites influence the oxidation resistance.

SEM studies

The SEM micrographs of the composites as such and the composites oxidized at 800 °C are given in Fig. 3b–f. The SEM of SiC derived by reacting Si and CB at 1,400 °C in argon is also given for comparison in Fig. 3a. It is seen from Fig. 3d that composites developed with GC–Si–B_4C (Batch D-1) contain SiC particles of the size 1–2 μm along with B_4C and carbon particles, whereas SiC nano rods and nano fibers were clearly seen in composites developed with Si and CB (Batch B-1) and sol–gel silica and CB (Batch C) as revealed by the SEM micrographs given in Fig. 3b and c, respectively, thereby showing that nano-SiC is incorporated in these composites. The size of the nano-SiC in composites developed using sol–gel-derived silica (Batch C, Fig. 3c) as Si source was much smaller (50-150 nm) as compared to the size of SiC in composites in which SiC is derived from Si and CB, Fig. 3b (150–300 nm). The branching of the rods was also visible in the composites developed with Si and CB (Batch B-1) and sol–gel silica and CB (Batch C) as nano-SiC precursors and the branching is attributed to the meeting of the ends of two nano rods, which can initiate the further growth of the nano rods from the junction [20]. The micrographs of the composites developed with GC–sol–gel silica–CB–B_4C (Batch C, Fig. 3c) showed nodules, which is attributed to the unreacted silica that also indicated that SiC formation was not complete in this composite that led to the weight loss of the composites at 1,000 and 1,200 °C (Table 6). The micrographs of SiC synthesized by the reaction between Si and CB (Fig. 3a, Batch A) and of the composites in which Si and CB (Fig. 3b, Batch B-1) were used as SiC precursor did not show CB, thereby, showing the complete reaction of Si and CB, which is in agreement with the X-ray result

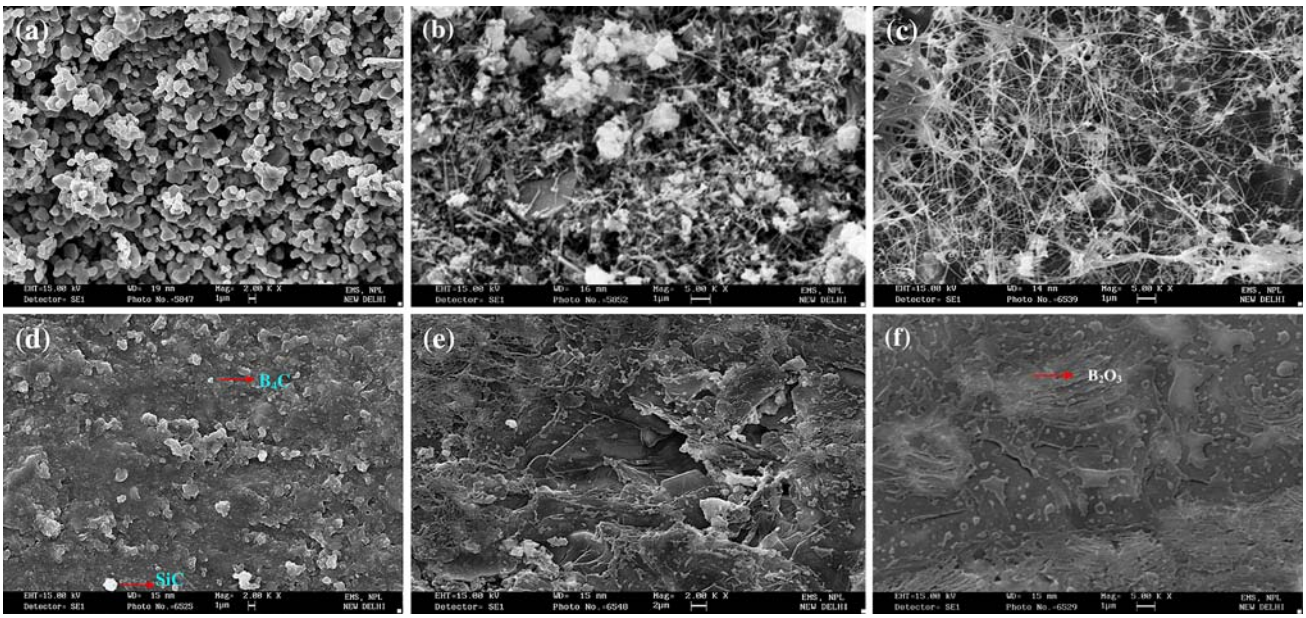

Fig. 3 Scanning electron micrographs of **a** Nano-SiC synthesized from carbon black and silicon (Batch A), **b** carbon–ceramic composite (Batch B-1, nano-SiC derived from Si and CB), **c** C–nano-SiC–B_4C (Batch C, nano-SiC derived from sol–gel silica and CB), **d** C–SiC–B_4C (Batch D-1, SiC is derived from Si and GC), **e** C–nano-SiC–B_4C (Batch B-1, nano-SiC derived from Si and CB) oxidized at 800 °C for 10 h, and **f** C–SiC–B_4C (Batch D-1, SiC derived from Si and GC) oxidized at 800 °C for 10 h

(Fig. 1a) that confirmed the complete reaction between CB and Si. It is also seen from the micrographs that SiC prepared by treating Si and CB (Fig. 3a, Batch A) showed only SiC nano particles of the size (80–700 nm) while in composites (Batch B-1) SiC nano rods are formed, which can be attributed to the catalytic effect of boric acid present in the commercial grade B_4C (Table 3). The GC, commercial Si, and B_4C powder contain other metallic impurities like iron (Tables 2, 3), which initiates the growth of SiC nano rods. It is also well known that boric acid acts as a catalyst in the carbo-thermal reduction of silica [18, 21] that proceeds through the formation of SiO as given in the following reaction

$$SiO_2(s) + C(s) \rightarrow SiO(g) + CO(g), \quad (5)$$

$$SiO(g) + 2C(s) \rightarrow SiC(s) + CO(g), \quad (6)$$

$$SiO(g) + 3CO(g) \rightarrow SiC(s) + 2CO_2(g), \quad (7)$$

$$3SiO(g) + CO(g) \rightarrow SiC(s) + 2SiO_2(s), \quad (8)$$

$$CO_2(g) + C(s) \rightarrow 2CO(g), \quad (9)$$

The overall reaction is

$$SiO_2(s) + 3C(s) \rightarrow SiC(s) + 2CO(g). \quad (10)$$

The reaction given in Eq. 5 is the crucial step and a solid–solid reaction [19–21]. In the present investigation, commercial Si employed as SiC precursor melted around 1,400 °C and reacted with surface oxygen present in CB to give SiO, which reacted with carbon to give SiC [22]. It may be mentioned here that the presence of SiC nano fibers in the sol–gel-derived SiC is due to the nano sized silica obtained through sol–gel process, which reacted with CB containing nano sized carbon particles to give SiC nano fibers. It was reported by the authors in the earlier communications that the sol–gel-derived silica blended with poly carbonate, polyphenylene oxide–polystyrene (PPO–PS) blended polymer and pitch on heat treatment to 1,400 °C in argon yielded SiC nano fibers and nano rods [23–25].

The SEM of the composites (Batch B-1 and D-1) oxidized at 800 °C (Fig. 3e, f) showed the formation of glassy B_2O_3. Oxidation of B_4C starts around 500 °C to form glassy B_2O_3 and the complete decomposition takes place around 800 °C. The formation of glassy layer over the SiC nano rods was also seen in the oxidized composites (Fig. 3e) developed with GC–Si–CB–B_4C (Batch B-1). The glassy B_2O_3 covered the surface of the composites and being impermeable to oxygen prevented the oxidation.

TEM analysis

Transmission electron microscope photographs of SiC synthesized with CB and Si (Batch A) and the composite developed with GC–Si–CB–B_4C (Batch B-1) is given in Fig. 4a–c. It is seen from Fig. 4a that the nano-SiC particles having the size of 15–80 nm were present in the nano-SiC synthesized by the reaction between Si and CB (Batch A). It is also observed that neither nano rods nor nano fibers were seen in the sample. The TEM of the composite (Batch B-1,

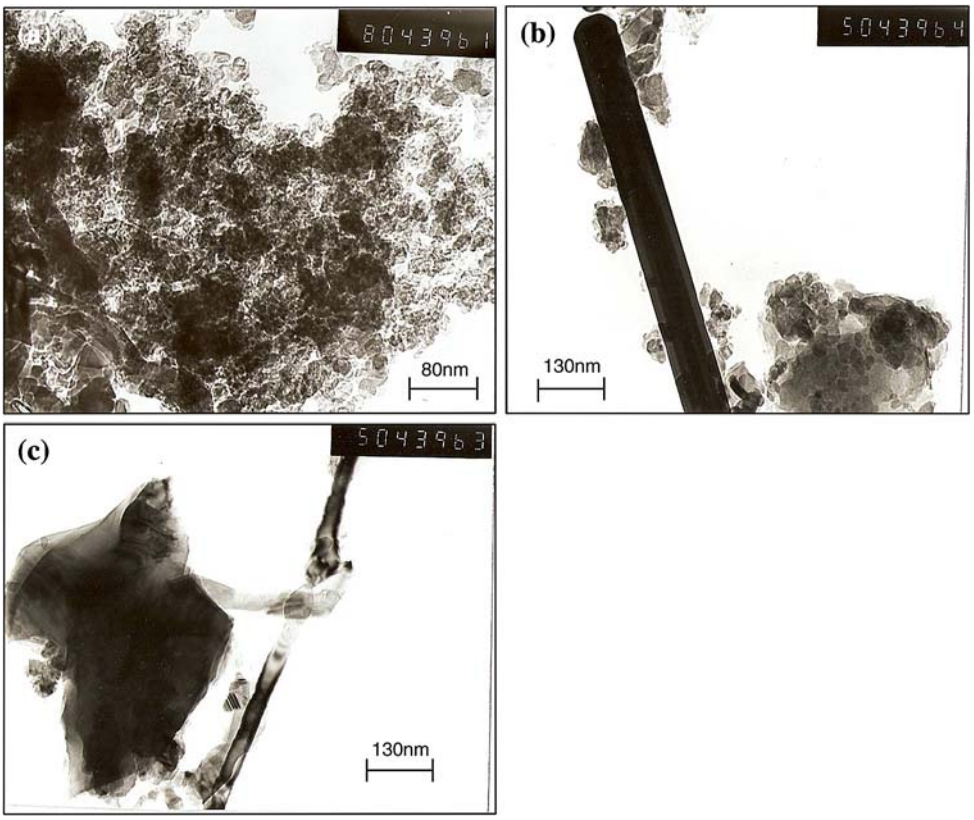

Fig. 4 Transmission electron micrographs of **a** Nano-SiC synthesized from carbon black and silicon (Batch A) and **b** and **c** C–nano-SiC–B_4C (Batch B-1, nano-SiC derived from Si and CB)

Fig. 4b) showed nano rods having diameter in the range 50–130 nm. These nano rods showed the stacking faults, which are generally seen in nano-SiC and in SiC whiskers [26]. The TEM of the SiC and the composites (Fig. 4a, b, c) did not show CB or Si, which is in close agreement with the SEM and X-ray results that excluded the presence of excess of CB and Si.

Conclusion

Nano-SiC incorporated composites (C–nano-SiC–B_4C) could be developed by employing CB and Si as well as sol–gel silica and CB as SiC precursors, whereas micro-SiC incorporated composites were developed using GC-derived carbon and Si and SiC particulates. The oxidation resistance studies of the nano-SiC incorporated composites (from CB or sol–gel silica) and of the composites developed by using Si and GC as micro-SiC precursor and also by using micro-SiC particulate showed that nano sized SiC influenced the oxidation of composites and exhibit better oxidation resistance at 800–1,000 °C as compared to the composites, which have micron sized SiC. The sol–gel-derived composite were unable to protect oxidation at 1,000 and 1,200 °C due to the incomplete formation of SiC.

Acknowledgement The authors are thankful to Dr. Vikram Kumar, Director, National Physical Laboratory, New Delhi, for his keen interest in the work and kind permission to publish the results and to Dr. A. K. Gupta, Head, Division of Engineering Materials, for his encouragement throughout this investigation. Thanks are due to Mr K.·N. Sood, Dr. A. K. Srivastava and Dr. S.·K. Halder for their valuable help in SEM, TEM, and X-ray studies, respectively. The authors also thank Department of Science and Technology, New Delhi for sanctioning the project on carbon–ceramic composites and also for the grant of project assistanceship to Mr. Sandeep Kumar.

References

1. Fitzer E (1987) Carbon 25:163
2. Mckee DW (1986) Carbon 24:737
3. Lee YJ, Radovic LR (2003) Carbon 41:1987
4. Shimada S, Sato T (2002) Carbon 40:2469
5. Feng HJ, Rong ZX, Jun LH, Bo XX, Wei FY, Min H (2004) J Mater Sci 39:7383. doi:10.1023/B:JMSC.0000048756.96547.bf
6. Ogawa I, Kobayyashi K, Nishikawa S (1988) J Mater Sci 23:1363. doi:10.1007/BF01154601
7. Kobayyashi K, Maeda K, Sano K, Uchiyama H (1995) Carbon 33:397
8. Raman V, Bhatia G, Aggrawal RK, Sengupta PR, Mishra A (2002) J Mater Sci Lett 21:317
9. Raman V, Bhatia G, Mishra A, Sengupta PR, Saha M, Rashmi (2005) Mater Sci Eng A 412:31
10. Prabhakaran PV, Sreejith KJ, Swaminathan B, Packirisamy S, Ninan KN (2009) J Mater Sci 44:528. doi:10.1007/s10853-008-3087-y
11. Guo Q, Song J, Liu L, Zang B (1999) Carbon 37:33

12. Mckee DW, Sipro L, Lamby EJ (1984) Carbon 22:507
13. Vaben R, Stover D (1994) J Mater Sci 29:3791. doi:10.1007/BF00357350
14. Zhang WG, Cheng HM, Sano H, Uchiyama Y, Kobayyashi K, Zhou IJ, Zhen ZH, Zhou BL (1996) Carbon 36:1591
15. Quanli J, Haijun Z, Suping L, Xiaolin J (2007) Ceram Int 33:309
16. Sogabe T, Matsuda T, Kuroda K, Hirahata Y, Hino T, Yamashina T (1995) Carbon 33:1783
17. Guo Q, Song J, Lui L, Zhang B (1998) Carbon 36:1597
18. Raman V, Parashar VK, Dhakate SR, Bahl OP, Dhawan U (2000) J Am Ceram Soc 83:952
19. Raman V, Parashar VK, Dhakate SR (2002) J Sol-Gel Sci Technol 25:175
20. Lia HJ, Lia ZJ, Mengc AL, Lia KZ, Zhangc XN, Xub YP (2003) J Alloys Compd 352:279
21. Raman V, Parashar VK, Bahl OP (1997) J Mater Sci Lett 16:1252
22. Larpkiattaworn S, Ngernchuklin P, Khongwong W, Pankurddee N, Wada S (2006) Ceram Int 32:899
23. Raman V, Bhatia G, Bhardwaj S, Srivastava AK, Sood KN (2005) J Mater Sci 40:1521. doi:10.1007/s10853-005-0596-9
24. Raman V, Bhatia G, Mishra AK, Bhardwaj S, Sood KN (2006) Mater Lett 60:3906
25. Raman V, Bhatia G, Sengupta PR, Srivastava AK, Sood KN (2007) J Mater Sci 42:5891. doi:10.1007/s10853-006-1175-4
26. Tjong SC, Chen H (2004) Mater Sci Eng R 45:1